

Ink Manifold Design of Phase Change Piezoelectric Ink Jets

Sharon S. Berger, Ronald F. Burr, James D. Padgett and David A.Tence
Tektronix, Inc., Color Printing and Imaging Division
Wilsonville, Oregon

Abstract

Full-width printheads offer many advantages for high speed office printers (e.g. the Tektronix Phaser® 350 solid ink printer). However, full width phase change printhead designs offer unique design challenges. In particular, manifold fluid acoustic time scales are often similar to individual jet resonant or driving time scales. The interaction can cause print quality and jet robustness issues. In addition to fluid interactions, structural interactions are often encountered. Market demand for higher print speeds requiring higher jet densities and higher firing frequencies only increase the manifold design problem. Conversely, advances in manifolding technology (i.e. smaller sizes) can be an enabling technology in the race for higher density and frequency, as individual jet size can be decreased. This paper will describe the models used to aid the integrated manifold design process. The first model used is a straightforward calculation of the steady-state pressure loss. The second model simulates the transient response of the manifold. The model includes manifold fluid acoustics, individual jet dynamics and fluid/structural interactions. The governing equations, model structure, and numerical method for this model will be discussed. The model is then validated by comparison to experimental data obtained on a production full-width design (the Phaser® 350 printer).

Introduction

Ink jet printer architectures consist basically of two types. The most prevalent is the shuttling printhead architecture. A small ink jet printhead shuttles quickly back and forth across the print media as it travels past the printhead and through the machine. In the non-shuttling architecture, the print media is moved quickly past the printhead, which has limited travel. To meet the needs of high speed printing for color printers in a shared work group environment, the non-shuttling architecture having a full width printhead was the chosen approach for its speed advantages.

In this architecture, individual jets are uniformly distributed in rows along the width of the print head. Individual jets arranged in arrays in the jet stack require ink to be delivered from the reservoir through ink feeds and distributed to all jets in the head along a manifold (Fig. 1). In order to maintain optimum print quality while printing on a curved surface, the jet rows are packed as close as possible to each other in the vertical direction. Fig. 2 illustrates a typical layout of individual jets and feed manifolds in a jet stack for two rows of jets. As demonstrated in Fig. 2, packing the jets closely requires the manifolds feeding ink to the individual jet inlets be outboard of at least one other color row of jets. As a result, minimizing individual jet size is a trade-off against maximizing the size and performance of the feed manifolds.

The mass flow rate of ink through the print head largely influences the required size of the ink distribution system which must be designed to meet steady-state flow, jet start-up conditions and acoustic cross-talk. The steady-state and transient pressure losses during printing must remain below the pressure drop that can be maintained by the jet meniscus and, ideally, below what can be seen as adverse print quality effects. Reduction of the pressure loss in the manifolds by increasing size or increasing the number of ink feeds to the manifold must be balanced by the increased cost and complexity or decreased jetting frequency.

An order of magnitude estimate of the start-up pressure fluctuation can be obtained by treating the manifold as a 'lumped mass' from which fluid is extracted by the jets without replenishment during the initial start-up (acoustic wave propagation) period. An estimate for the pressure change during this time period can be obtained as follows:

$$\Delta P \approx a^2 \frac{mjets}{Vman} \approx 40{,}000 \text{ Pa},$$

where

a	fluid sound speed
mjets	mass ejected at one firing
Vman	manifold volume

The above pressure drop could not be realistically sustained by the jet meniscus (the pressure drop to overcome surface tension is approximately 1500 Pa) and a more detailed analysis which accounts for the fluid interaction between the manifold and jets is required. This estimate does, however, clearly indicate the significant magnitude of pressure fluctuations that may be generated in the inlet manifold during the start-up.

It is often found that the acoustic time scales for a manifold section are similar to the jet driving time scales and significant interaction takes place. The natural

frequency (f) of the Phaser® 350 printer manifold is given below (a is ink sound speed, L is manifold length).

$$f = \frac{a}{4*L} \approx 10 \text{ kHz}$$

The Phaser® 350 printer operates at firing frequencies of 8 and 11 kHz. Since the individual jet and manifold frequencies are similar, it is anticipated that the transient (acoustic) response of the manifold may influence the individual jet performance if the pressure fluctuations are of significant magnitude. Fig. 3 illustrates the connection between manifold frequency and the potential affect on jet performance. This figure is the output of a lumped parameter model of an individual jet viewed from the jet inlet. From this model of a typical ink jet, we can see that the jet is sensitive to low frequencies (in the range of 2 to 5 kHz).

The remainder of the paper will be devoted to describing two manifold models (steady-state and transient) and then showing how the the models were validated and used in the design process. Details of the models include derivation of the governing equations and treatment of interactions with individual jets and other geometries. An example of how the models were used to model a particular geometry, and comparison of experimental and theoretical results will be presented.

Steady State Pressure Loss Model

One criteria in determining manifold performance is the steady-state pressure loss encountered when all jets are firing. This pressure loss can result in degradation of nominal jet performance and if too high will result in jet starvation and robustness issues. To determine the steady state pressure loss a resistance flow model is used. The model takes advantage of the symmetry of the jet stack as is shown in Fig. 1 by modeling only one feed and one sixth of the manifold. The calculation of the pressure loss is shown below

$$\Delta P = R_f \dot{m} + \int R_m \dot{m}(x)dx$$

where R_f is the feed resistance and R_m is the manifold resistance

In this equation, the resistance is calculated using the analytical fully-developed viscous flow equations as derived in White (Ref. 3).

$\Delta P = R\dot{m} = \frac{128\mu c}{\rho\pi a^4}\dot{m}$ for circular ducts, where a and c are duct diameter and length, respectively

$$\Delta P = R\dot{m} = \left(\frac{\mu}{\rho}\right)\left(\frac{12c}{a^3 b}\right)\left(1 - \frac{192a}{\pi^5 b}\sum_{j=1,3,5}\frac{\tanh\left(\frac{j\pi b}{2a}\right)}{j^5}\right)^{-1}$$

for rectangular ducts where a, b, and c represent duct height, width, and length, respectively

The maximum flow is calculated by multiplying the number of jets by the individual jet drop mass by the maximum firing frequency. Along the manifolds, this flow rate changes at it moves down a manifold due to removal by the jets. The flow is integrated along the manifold to account for the reduction in flow rate.

From the pressure loss equation, steady state pressure loss can be determined along the manifold. This steady state pressure loss can be related to jet performance using experimental data such as that shown in Fig. 4. This figure illustrates the effect of steady state pressure loss on flight time. Print quality artifacts can be seen with differences in flight time of about 25 µs or more. The performance data establishes the maximum pressure loss acceptable and thus the governs the required manifold size for steady state pressure loss. Designs must accommodate both the manifold size requirements and individual jet sizing requirements.

Manifold Model Development

Once the required manifold size to meet steady-state pressure loss has been determined, the transient response of the manifolds must be evaluated. In this section the model used in the transient design of the ink feed manifolding is discussed.

The simplified one-dimensional analysis below considers the dynamic (acoustic) response of the manifold when all jets are started simultaneously. The model accounts for the acoustic behavior in the manifolds, the interaction with the individual jet fluid components and the fluid-structure interaction with the jet stack plates.

In developing the governing equations, a fluid manifold element control volume is considered. Governing differential equations are obtained from conservation of mass and momentum, respectively, with the acoustic flow assumption of small perturbations applied. The effects of variable area ($c_A u$), fluid viscosity ($c_\mu u$) and mass flow due to individual jets ($m_d + m_f$) are also included.

$$\frac{\partial p}{\partial t} + \rho a^2 \frac{\partial u}{\partial x} + c_A u = -\frac{a^2}{AL}(m_d + m_f)$$

$$\frac{\partial u}{\partial t} + \frac{1}{\rho}\frac{\partial p}{\partial x} + c_\mu u = 0$$

As mentioned above, in addition to the manifold fluid acoustics the model also includes mass flow terms due to individual jets. The jet flow source term (m_d) from the manifold is an approximation of the flow into the jet inlet while the jet is firing. This term can also be used to find the natural resonance of the manifold system by using an step function as input. The second term, m_i, is used to simulate the dynamic response of the jets caused by the pressure fluctuations induced in the manifold. A simple lumped parameter model (Fig. 5) is used to model the jet. This jet model simulates the effect of the internal fluid features, meniscus and piezoelectric driver as combined resistive, inductive and capacitive elements. These contributions from the individual jets are continually distributed (i.e. homogeneous) along the manifold model segment.

Another element of the manifold model is its ability to model the fluid/structure interaction in the manifolds. This is mainly used to model compliant features along the manifold walls (see Fig. 6) and is motivated by the desire to decrease the pressure fluctuations induced in the manifold. Using plate deflection theory (Ref. 4), an estimate of deflection due the pressure gradient can be made. This deflection of the wall into an air gap essentially increases the capacity of the manifold. This increased capacity can be modeled as extra manifold compliance, which has the effect of decreasing sound speed. The derivation of effective sound speed for a square diaphragm follows.

diaphragm compliance : $$C_d = \frac{\rho h^5 (1-\nu^2)}{60 E \delta^3}$$

fluid compliance : $$C_a = \frac{h \cdot w}{a^2}$$

effective compliance : $$C_{eff} = C_d + C_a$$

sound speed correction : $$a_r = \sqrt{\frac{1}{1+\frac{C_d}{C_a}}}$$

effective sound speed : $$a_{eff} = a_r \cdot a$$

Figures 7a and b illustrate the relationships of capacitance and effective sound speed with compliant wall geometry. The critical feature, height, is varied.

The governing differential equations are hyperbolic (wave) in nature. A finite-difference method is used to solve these equations. Because of the hyperbolic nature, a flux vector splitting upwind scheme is used. The characteristic equations are integrated in the domain interior using a predictor-corrector finite-difference scheme upwinded according to the sign of the eigenvalue. Total variational diminishing (TVD) schemes have also been used, but the additional computational effort is not usually justified due to the damping behavior of the individual jets distributed along much of the manifold. A Runge-Kutta numerical scheme is used to integrate the homogenized individual jet models at each node of the manifold. Initial conditions are assumed to be uniform (zero) pressure and velocity. Boundary conditions are required at both ends of each manifold segment and correspond to either an infinite reservoir (constant pressure supply), zero velocity capped end or an interconnection to one or more other segments in the manifold feed system.

The model is designed to be very flexible and modular. Each segment can have any boundary condition mentioned above, as well as have active or passive jets (passive jets simulate non-firing jets which contain only the dynamic contributions of the jets) The user has several options for adding compliance. Compliance from a flexible wall or diaphragm can either be entered by specifying geometry (and using the effective sound speed calculation) or by directly entering the sound speed. Segments are pieced together with the desired boundary conditions to model the complete manifold system (see Fig. 8).

Application and Results

The response that was used to design the manifolds of the Phaser® 350 printer was orifice displacement. This response is the response of the jet meniscus to the pressure fluctuation in the manifolds. This was found to be the best response as the individual jets were able to provide significant damping and filtered some of the fluctuations in the manifolds. Comparison of model results and jet flight time showed that a criteria of 70 ng displacement was determined acceptable (see Fig. 9). This displacement correlates about one third of an orifice volume.

Fig. 10 shows typical results for a manifold simulation. Both a low frequency response associated with the manifold and feed interaction and a high frequency response associated with jet operation are present. In the Phaser® 350 printer, the spectral responses have been intentionally separated in order to reduce unwanted artifacts and cross-talk in high flow rate printing. It is noted that the primary source of damping for the acoustic wave along the manifold is provided by the interaction with the individual jets distributed along the manifolds. Viscous damping along the manifold is negligible in comparison. Fig. 11 shows the results of scanned print intensity values from a Phaser® 350 printer. Comparing the amount of damping between the model and the scanned data, it is clear that the model does not provide an adequate level of damping.

In designing the manifold for the Phaser® 350 printer, the model showed that unless other flexibilities were present in the system (passage walls, air bubbles, etc.) that significant pressure fluctuations would be generated at the individual ink jet inlet. Using the model, a design was implemented that had additional compliance in the manifolds. This reduced the magnitude of fluctuations at the jet meniscus by 70%.

Conclusions

With any head architecture, full-width or smaller, that has manifolds feeding individual jets, the problem of steady state pressure loss and jet start-up has the potential to exist.

As jet firing frequencies become faster, the problem of interaction between manifold and jet frequencies applies to the smaller heads as well. Manifold design issues in all cases are compounded with increased jet densities. With no reduction in demand for higher print speeds, the ability to integrate the manifold and jet design and improve manifolding technology remains critical to success.

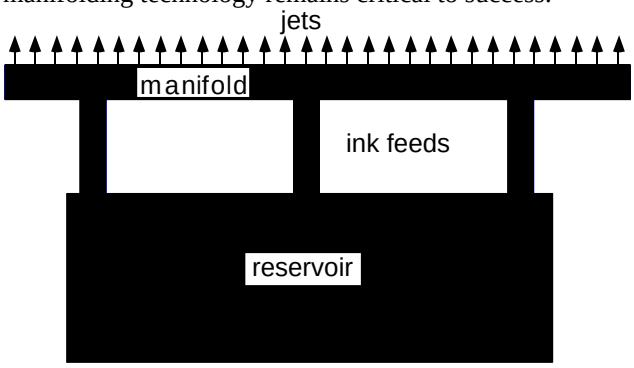

Figure 1. Jet Manifolding Schematic

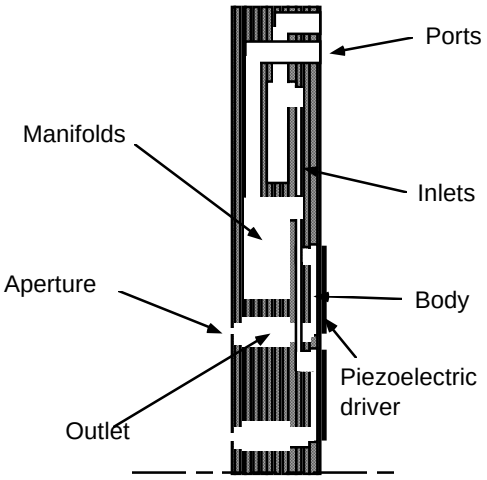

Figure 2. Typical Jet Stack Layout

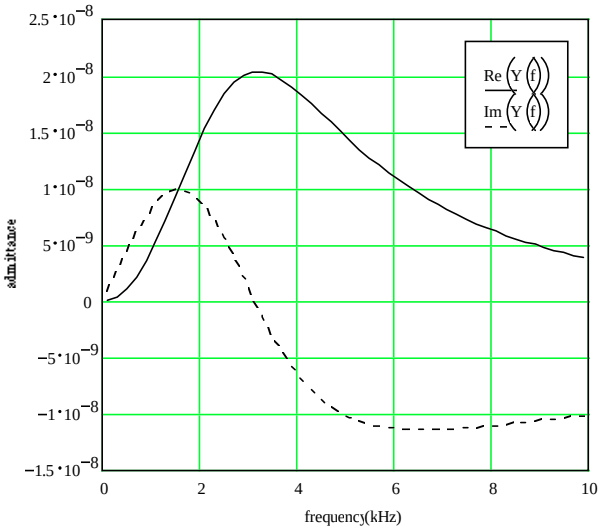

Figure 3. Jet Admittance to Manifold Pressure

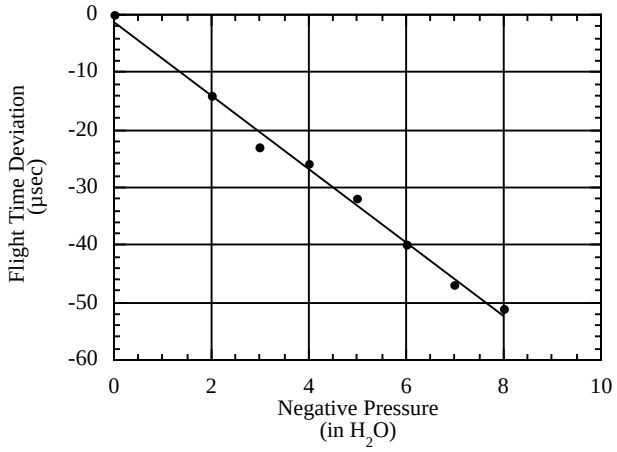

Figure 4. Pressure Loss Effects on Flight Time

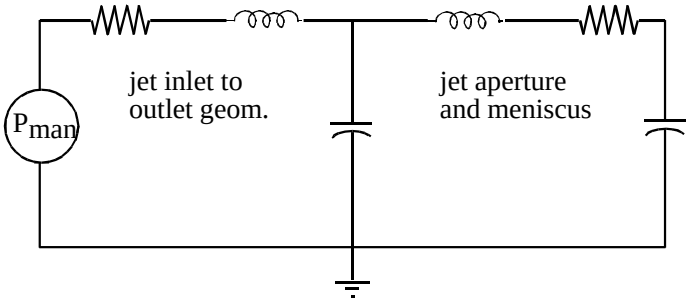

Figure 5. Simple Jet Lumped Parameter Model

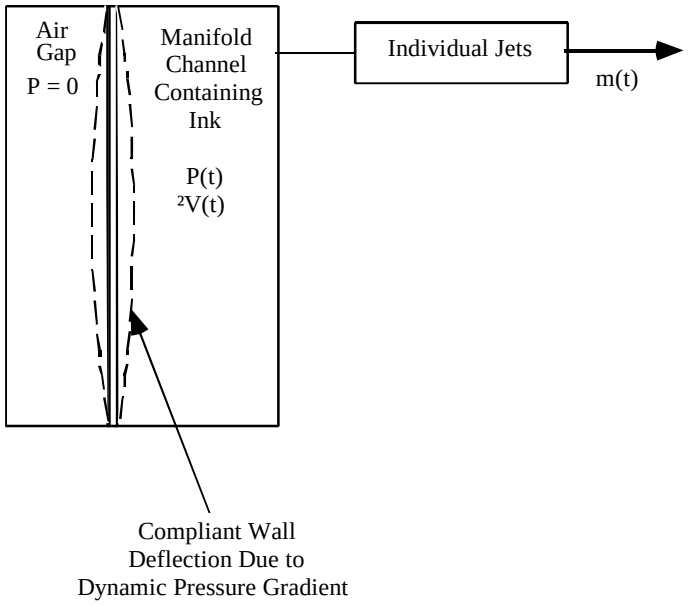

Figure 6. Structural Compliance Model

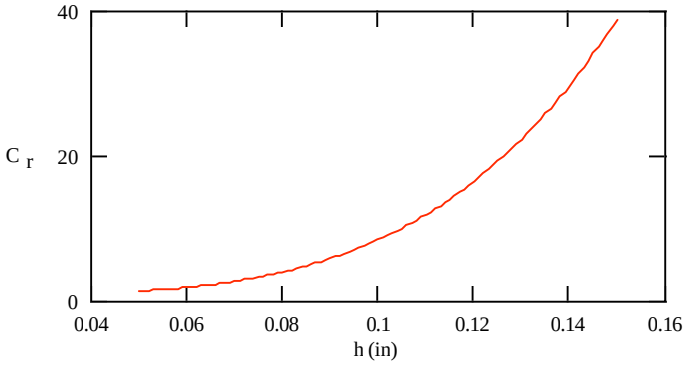

Figure 7a. Manifold Compliant Wall Height Effects on Capacitance Ratio (effective/fluidic)

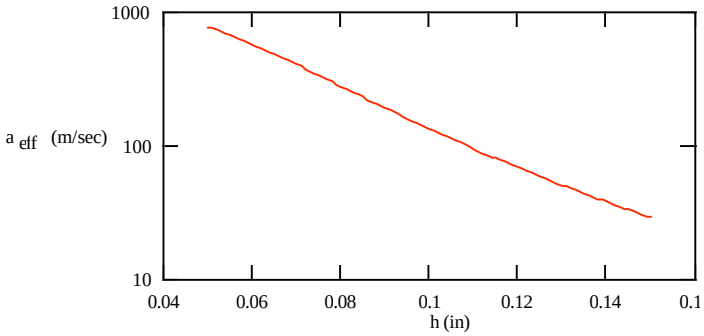

Figure 7b. Manifold Compliant Wall Height Effects on Effective Sound Speed

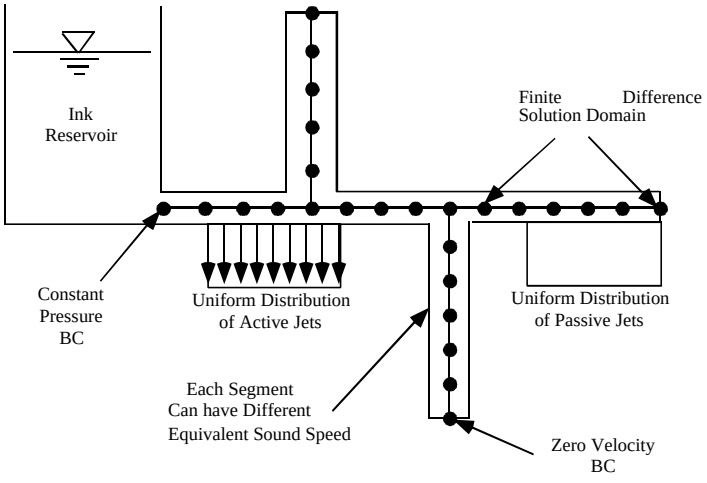

Figure 8. Manifold Model Building Blocks

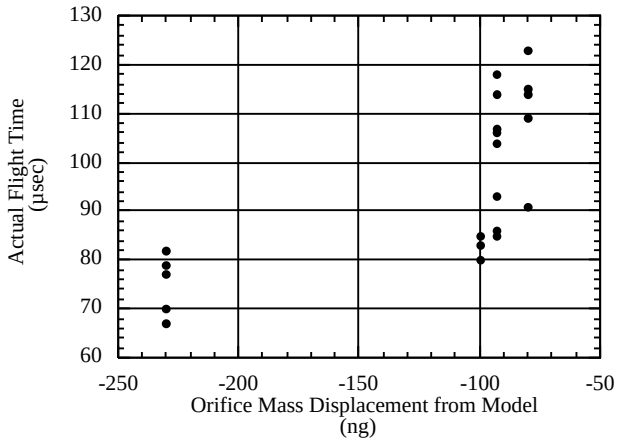

Figure 9. Model Correlation to Performance

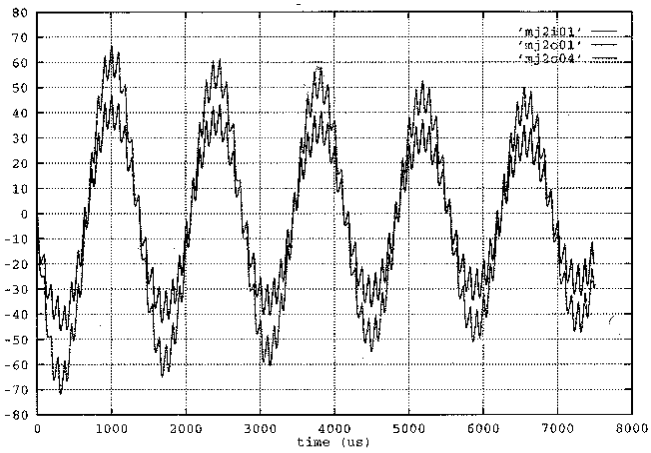

Figure 10. Phaser® 350 Printer Manifold Simulation

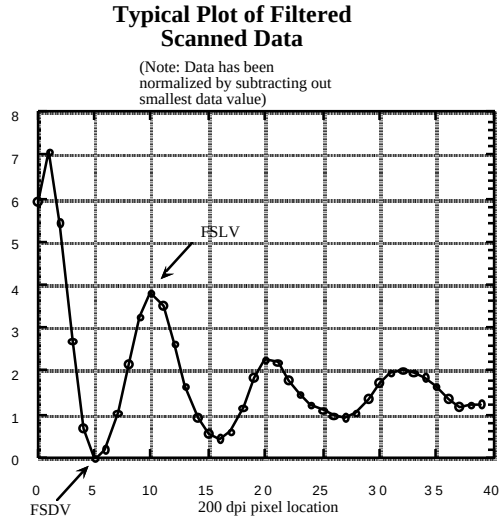

Figure 11. Phaser® 350 Printer Experimental Data

References

1. “Overview of Phase Change Piezoelectric Ink Jet Fluids Modeling and Design”, Burr, R.F, S.S. Berger, D.A. Tence, FED-Vol. 239, Proceedings of the ASME, 545-552.

2. Currie, I.G., Fundamental Mechanics of Fluids, McGraw-Hill, New York, 1974.

3. White, F.M., Viscous Fluid Flow, McGraw-Hill, New York, 1974.

4. Timoshenko, S., Theory of Plates and Shells, 2nd Ed., McGraw-Hill, New York, 1987.